



1

2 **Mercury emissions of a coal fired power plant in Germany**

3

4 **Andreas Weigelt^{1,*}, Franz Slemr², Ralf Ebinghaus¹, Nicola Pirrone³, Johannes**
5 **Bieser^{1,4}, Jan Bödewadt¹, Giulio Esposito³, Peter F.J. van Velthoven⁵**

6 ¹Helmholtz-Zentrum Geesthacht (HZG), Institute of Coastal Research, Geesthacht, Germany

7 ²Max-Planck-Institute for Chemistry (MPI-C), Department of Atmospheric Chemistry,
8 Mainz, Germany

9 ³National Research Council (CNR), Institute of Atmospheric Pollution Research, Rende, Italy

10 ⁴Deutsches Zentrum für Luft- und Raumfahrt (DLR), Institute of Atmospheric Physics,
11 Oberpfaffenhofen, Germany

12 ⁵Royal Netherlands Meteorological Institute (KNMI), Chemistry and Climate Division, De
13 Bilt, Netherlands

14 *now at: Federal Maritime and Hydrographic Agency (BSH), Hamburg, Germany

15 Correspondence to: A.Weigelt (Andreas.Weigelt@bsh.de), F. Slemr (franz.slemr@mpic.de)

16

17 andreas.weigelt@bsh.de

18 franz.slemr@mpic.de

19 ralf.ebinghaus@hzg.de

20 pirrone@iia.cnr.it

21 johannes.Bieser@hzg.de

22 jan.boedewadt@hzg.de

23 esposito@iia.cnr.it

24 velthove@knmi.nl

25



1 Abstract

2 Hg/SO₂, Hg/CO, NO_x/SO₂ emission ratios (ERs) in the plume of coal fired power plant
3 (CFPP) Lippendorf near Leipzig in Germany were determined within the European
4 Tropospheric Mercury Experiment (ETMEP) aircraft campaign in August 2013. GOM
5 fraction of mercury emissions was also assessed. Measured Hg/SO₂ and Hg/CO ERs were
6 within the measurement uncertainties consistent with the ratios calculated from annual
7 emissions in 2013 reported by the CFPP operator, the NO_x/SO₂ ER was somewhat lower.
8 GOM fraction of total mercury emissions, estimated by three independent methods, was
9 ~10% with an upper limit of ~25%. This result is consistent with findings by others and
10 suggests that GOM fractions of ~40% of CFPP mercury emissions in current emission
11 inventories are overestimated.

12

13 1 Introduction

14 Mercury and especially methyl mercury which bio-accumulates in the aquatic nutritional
15 chain are harmful to humans and animals (e.g. Mergler et al., 2007; Scheuhammer et al.,
16 2007; Selin, 2009; and references therein). Therefore, its emissions are on the priority list of
17 several international agreements and conventions dealing with environmental protection and
18 human health, including the United Nations Environment Program (UNEP) Minamata
19 convention on mercury (www.mercuryconvention.org). Mercury is emitted to the atmosphere
20 from a variety of natural (e.g. volcanic activity, evaporation from ocean and lakes) and
21 anthropogenic sources (e.g. coal and oil combustion) (Mason et al., 2009; Pirrone et al.,
22 2010). Coal-fired power plants (CFPPs) are believed to account for most ($\geq 56\%$) of mercury
23 emitted by stationary combustion sources which constitute 35 – 77% of all anthropogenic
24 emissions (Pirrone et al, 2010; Chen et al., 2014; Ambrose et al., 2015).

25 Mercury from CFPPs is emitted as gaseous elemental mercury (GEM), gaseous oxidized
26 mercury (GOM) and particulate bound mercury (PBM). Elemental mercury has a high vapour
27 pressure, is virtually insoluble in water resulting in a long residence time in the atmosphere of
28 about 1 yr (Selin, 2009). GOM with its high solubility and low vapour pressure is readily
29 washed and rained out as are the particles carrying particulate mercury (PM). GOM and PM
30 are believed to be in equilibrium (Rutter and Schauer, 2007; Amos et al., 2012). GOM is thus
31 a major driver for the global mercury deposition and is estimated to make up more than 50%
32 of the total Hg deposition (Zhang et al., 2012a; Bieser et al., 2014).



1 There are only two sources of GOM in the atmosphere: primary GOM emissions from
2 anthropogenic sources and the oxidation of elemental mercury. The major anthropogenic
3 mercury sources on a global scale are small scale artisanal gold mining (SSAG) and coal
4 combustion (Pirrone et al. 2010). While SSAG emits solely elemental mercury, the CFPP
5 emissions in emission inventories are estimated to have a GOM fraction between 35% and
6 40% (Pacyna et al., 2006; Wilson et al., 2010; EPA, 2011). However, global and regional
7 model studies have repeatedly indicated that models are overestimating atmospheric GOM
8 concentrations (Zhang et al., 2012b; Kos et al., 2013; Bieser et al., 2014). Possible
9 explanations for this are an overestimation of the GEM oxidation rates or the overestimation
10 of the amount of GOM emitted by CFPPs. The latter has been hypothesized to be due to a fast
11 reduction of GOM inside the plume (Zhang et al., 2012b; Kos et al., 2013).

12 While the operators of CFPPs are forced to measure and report the amount of mercury
13 released into the atmosphere, there is only little knowledge on the speciation of these
14 emission sources. That is because of varying composition of burnt coal, complex chemistry in
15 the stack gases (e.g. Schofield, 2008; Ernest Tatum et al, 2014) and the large number of
16 different methods used to clean CFPP flue gases with very different percentage of gaseous
17 oxidized mercury (GOM) to total mercury ranging from less than 10% up to 90% (Wang et
18 al., 2010, Schuetze et al., 2012, and references therein). Analytical problems also contribute to
19 the uncertainty: the current emission monitoring systems are not sensitive enough to measure
20 and speciate low mercury concentrations in flue gases of modern CFPPs (Mayer et al., 2014).
21 Moreover, there has been evidence that the current ambient air measurement systems might
22 not capture all oxidized mercury species with similar efficiency (Jaffe et al., 2014; Gustin et
23 al., 2015a, Weiss-Penzias et al., 2015).

24 The European Tropospheric Mercury Experiment (ETMEP) was carried out in July/August
25 2012 (ETMEP-1) and August 2013 (ETMEP-2) to measure local emissions, vertical profile
26 from inside the boundary layer to the lower free troposphere, and horizontal distribution of
27 mercury over Europe. In total 10 measurement flights were performed over Italy, Slovenia,
28 and Germany with two propeller aircraft. The ETMEP-1 campaign focused on volcanic
29 emissions of Etna. The objectives of the ETMEP-2 campaign were a) to obtain vertical
30 mercury profiles above several sites in central and southern Europe (Weigelt et al., 2016), b)
31 to assess horizontal distribution of mercury concentrations during the flight from Italy to



1 Germany, and c) to determine mercury emission ratios for a coal-fired power plant (CFPP)
2 near Leipzig. Here, we present the measurements of CFPP emissions and their speciation.

3

4 **2 Experimental**

5 The power plant under investigation is located in Lippendorf, a small village ca 15 km south
6 of Leipzig. The CFPP of Lippendorf consists of two units with 934 MW gross power each. It
7 has been in operation since 2000 and belongs with a net efficiency of 42.6% to one of the
8 most modern and efficient CFPPs in Europe. About 10 million metric tons of brown coal with
9 rather high sulphur content from a nearby open pit mine are burnt annually. The SO₂
10 emissions are reduced by flue gas desulfurization (FGD) system using wet washing with CaO
11 suspension. Despite the efficient FGD cleaning, the CFPP of Lippendorf ranks 4th most
12 harmful emitter in Germany (Preiss et al., 2013) and 14th most harmful emitter in Europe
13 according to the European Environment Agency (EEA, 2011) with respect to health. Annual
14 emissions reported by the operator of the CFPP Lippendorf for 2013, the year of our
15 measurements, were: $1.18 \cdot 10^{13}$ g CO₂, $1.21 \cdot 10^{10}$ g SO₂, $7.91 \cdot 10^9$ g NO_x, $7.55 \cdot 10^8$ g CO, and
16 $4.1 \cdot 10^5$ g Hg, among other pollutants. Mercury limit emission values (LEVs) of large
17 combustion plants in Germany are stipulated by ordinance (Federal Law) from 2004 and its
18 revision in 2013 to 50 µg m⁻³ as a half hour average, 30 µg m⁻³ as a daily average, and 10 µg
19 m⁻³ as an annual average (Mayer et al., 2014). Continuous monitoring of mercury emissions is
20 mandatory but only annual total (unspeciated) mercury emissions have to be reported.

21 The measurement campaign described above was performed with a CASA 212 two engine
22 turboprop aircraft (Fig. 1a) operated by Compagnia Generale Ripresearee
23 (<http://www.terraitaly.it>). The CASA 212 with a maximum payload of 2.7 tons can carry the
24 measurement instruments, different service instruments, the power supply, two pilots, and 5
25 operators. With a normal cruising speed of ~ 260 km h⁻¹ its range is ~ 1600 km. Although the
26 maximum flight level of the unpressurized aircraft is 8500 m, the maximum altitude of
27 ETMEP-2 flights without oxygen supply was limited to ~3000 m above sea level (a.s.l.),

28 The aircraft was equipped with a gas inlet system (Fig. 1b) which had been developed and
29 manufactured at the Helmholtz-Zentrum Geesthacht. The gas inlet was designed for the
30 cruising speed of the CASA 212 of ~ 72 m s⁻¹. A diffuser tube reduced the air speed to ~ 5 m
31 s⁻¹. About 120 l min⁻¹ (ambient conditions) enters the inlet at the cruising speed of 260 km h⁻¹.

32 The air sample is taken in the centre of the diffuser tube with a flow rate of ~ 25 l min⁻¹. The



1 remaining flow of 95 l min^{-1} is directed to the back of the inlet where the air speed is
2 increased by a nozzle and the air exits. By replacing the inlet and outlet nozzle with smaller or
3 larger ones, this inlet system can be fitted to other aircraft with a different cruising speed. In
4 the expanded area (behind the main sample line) the air temperature (T), static pressure (p),
5 and relative humidity (rH) are measured. To avoid adsorption losses of sticky trace gases, the
6 internal surface of the inlet system was coated with Teflon and only PFA tubing was used for
7 the sampling lines. The outside of the inlet was coated with copper to avoid electrostatic
8 charging. The inlet was fastened onto a 90 cm long telescope tube (6 cm diameter) which was
9 mounted in a hole on the floor fuselage via a sliding guide. After take-off, the tube was
10 pushed down by ~40 cm from inside the aircraft, to ensure that the inlet nozzle is outside the
11 aircraft boundary layer. Before landing the tube was pulled back into the aircraft to protect it
12 from damage by objects whirled up by the front wheel. The inlet and the telescope tube were
13 equipped with heaters to prevent icing but during the ETMEP measurements the heating was
14 always switched off because the measurement flights were carried out in summer at altitudes
15 below 3000 m a.s.l. The tubing from the inlet to instruments (~2.5 m long 3/8" main sample
16 tube with PFA manifolds to instruments) was not heated. The temperature inside the cabin
17 was 18 to 30°C.

18 The aircraft was equipped with three mercury measurement instruments: a Lumex
19 RA-915AM, a Tekran 2537B, and a Tekran 2537X (cf. Tab. 1). The Lumex RA-915 AM is
20 based on atomic absorption spectroscopy (AAS) with Zeeman background correction
21 (Sholupov et al., 2004) and as such measures specifically only gaseous elemental mercury
22 (GEM) with a temporal resolution of 1 s. Its raw signal is noisy (about $\pm 4 \text{ ng m}^{-3}$ with a
23 temporal resolution of 1 s) and is dependent on pressure and temperature. Nevertheless, the
24 fast response of the instrument is very useful to detect GEM in rather narrow highly
25 concentrated plumes at a cruising speed of about 72 m s^{-1} . Because of thermal drifts its zero
26 was measured every 4 min for 1 min.

27 The Tekran 2537B and 2537X analysers are based on preconcentration of mercury and its
28 compounds on gold traps (Slemr et al., 1979), thermodesorption, and detection by cold vapour
29 atomic fluorescence spectroscopy (CVAFS). Although CVAFS can detect only GEM,
30 mercury compounds are converted to GEM during adsorption or thermodesorption (Slemr et
31 al., 1978) and, consequently Tekran instruments measure total gaseous mercury (TGM). The
32 instruments use two gold traps to ensure a continuous measurement: while one is adsorbing



1 mercury during sampling, the other one is being analysed and vice versa. The highest
2 temporal resolution of the Tekran instruments of 150 s is given by the time necessary for the
3 thermodesorption of mercury from the gold traps and their cooling. The Tekran 2527X
4 analyser was run with quartz wool trap upstream of the instrument, which removes gaseous
5 oxidized mercury (GOM) and aerosol particles with particle bound mercury (PBM) but no
6 GEM from the air stream (Lyman and Jaffe, 2011; Ambrose et al., 2013). The Tekran 2537B
7 analyser was operated as backup instrument without a quartz wool trap. The Teflon made
8 (PFA and PTFE) aircraft gas inlet and tubing system are similar to the CARIBIC trace gas
9 inlet for which high GOM transmission was qualitatively demonstrated. Based on the short
10 residence time (0.3 sec) in the tubing to the instrument, the conditions as during an
11 international field intercomparison (Ebinghaus et al., 1999), and higher GOM concentrations
12 in the plume than in ambient air, we presume Tekran measurements without quartz wool trap
13 represent total gaseous mercury (TGM = GEM + GOM). Therefore, the Tekran 2537B
14 measurement are believed to represent TGM concentrations whereas those by Tekran 2537X
15 GEM concentrations, both with an uncertainty of 12.5%. The uncertainty has been calculated
16 by Weigelt et al. (2013) using two different approaches according to ISO 20988 type A6 and
17 ISO 20988 Type A2. This uncertainty complies with the quality objective of the EU air
18 quality directive 2004/107/EC. The instrumental setup in the aircraft was almost identical and,
19 therefore, we expect the uncertainty to be very similar.

20 Direct estimation of the GOM concentrations was made using three manual KCl denuder
21 samples taken during the vertical profiles (sampling time 1 hour or longer, sampling flow rate
22 6.4 l/min at standard temperature and pressure (STP; $T=273.15$ K, $p=1013.25$ hPa),
23 corresponding to ~ 10 l/min at ambient temperature and pressure in 3000 m a.s.l and
24 controlled using a mass flow controller): one downwind of the Lippendorf CFPP, one upwind
25 over the city of Leipzig (both on August 21, 2013), and one over the GMOS master site
26 “Waldorf” in northern Germany on August 22. Two blank samples were also taken by KCl
27 denuders handled exactly in the same way as the samples (denuder preparation, installation to
28 sampling setup, storage, analysis) but without sucking sample air through them. After all
29 flights had been finished, the KCl denuders were analysed for their total GOM loads in the
30 laboratory. Despite a relatively high uncertainty of about ± 5 pg m^{-3} , the method provides
31 semi-quantitative information about GOM concentration in the plume.



1 We note that both methods used here to estimate GOM concentrations are subject to
2 interferences. GOM captured by quartz wool can be released by higher air humidity (Ambrose
3 et al., 2015) and KCl traps and denuders can release GOM in presence of high ozone and
4 water concentrations (Lyman et al., 2010; Huang and Gustin, 2015). These interferences may
5 result in overestimation of GEM and underestimation of GOM emissions. GEM measured by
6 Lumex is not subject to any known interference.

7 For the identification and characterization of different air masses carbon monoxide (CO),
8 ozone (O₃), sulphur dioxide (SO₂), nitric oxide (NO), nitric dioxide (NO₂), and the basic
9 meteorological parameters temperature (T), pressure (p), and relative humidity (rH) were
10 measured simultaneously with high temporal resolution. Instrument details including the
11 estimated measurement uncertainty are summarised in Table 1. Uncertainties were calculated
12 according to the individual instrument uncertainty given by the manufacturer and the
13 calibration gas accuracy (CO, O₃, SO₂, NO). All instruments were protected from aerosols
14 using PTFE filters (0.2 µm pore size). Model meteorological data like potential vorticity,
15 equivalent potential temperature, relative and specific humidity, cloud cover, cloud water
16 content, three-dimensional wind vector, as well as five day backward trajectories were
17 calculated every 150 s along the aircraft flight tracks for additional information. These
18 calculations are based on meteorological analysis data from the European Centre for Medium-
19 Range Weather Forecasts (ECMWF) and the TRAJKS trajectory model (Scheele et al., 1996).

20 Before take-off all instruments were warmed up for at least 45 minutes, using an external
21 ground power supply. During the starting of the engines the power was interrupted for less
22 than 3 minutes. Since 45 minutes were too short to stabilize the Tekran 2537 internal
23 permeation source, these instruments were calibrated only after each measurement flight
24 before the engine shut down. All data were recalculated, using the post flight calibration. The
25 pressure in the fluorescent cells of both Tekran instruments was kept constant using upstream
26 pressure controllers at the exits of the cells. This eliminated the known pressure dependence
27 of the response signal (Ebinghaus and Slemr, 2000; Talbot et al., 2007). The Lumex analyser
28 has a much shorter warm up time of less than 10 minutes and was, therefore, calibrated before
29 take-off with the internal calibration cell. The CO instrument calibration takes 60 seconds and
30 was, therefore, performed during the measurement flights every 20 minutes with external
31 calibration gas. The O₃, SO₂, NO/NO₂ instruments have a fairly constant signal response and
32 were thus calibrated before and after the ETMEP-2 measurement campaign. Multipoint SO₂



1 and NO_x calibration was made using dilution (EnviroNics 300E calibrator) of certified
2 standard gases. NO₂ conversion efficiency was determined using gas phase titration. The
3 factory calibration was used for the pressure, temperature and relative humidity sensors. The
4 measurements were synchronized using their individual delay and response times. Please note
5 that all mercury (TGM, GEM, and GOM) concentrations are reported at standard temperature
6 and pressure (STP; T = 273.15K, p = 1013.25 hPa). At these standard conditions 1 ng m⁻³
7 corresponds to a mixing ratio of 112 ppqv (parts per quadrillion by volume).

8

9 **3 Vertical distribution and Hg/SO₂, Hg/CO, NO_x/SO₂ emission ratios**

10 The measurements were carried out on August 21 and 22, 2013. On August 21 between 9:30
11 and 11:20 UTC the aircraft flew many circles at different altitudes downwind of a CFPP
12 Lippendorf (51°11'N, 12°22'E) followed between 11:25 and 12:20 UTC by a vertical profile
13 upwind of CFPP Lippendorf over the city centre of Leipzig (51.353°N, 12.434 °E). Between
14 8:30 and 10:00 UTC of August 22 another vertical profile above the GMOS master site
15 “Waldhof” (52°48'N, 10°45'E, about 200 km from Leipzig on the line connecting Leipzig and
16 Hamburg) was flown, followed between 10:00 and 10:35 UTC by additional measurements
17 downwind of the CFPP Lippendorf. Each vertical profile consists of at least seven horizontal
18 flight legs, consisting of circles and altogether lasting 5 - 10 minutes each. The flight legs
19 started inside the boundary layer at about 400 m above ground and ended at 3000 m a.s.l. The
20 tracks of the flight in the CFPP plume on August 21 and August 22 are shown in Figure 2a
21 and 2b, respectively. The CFPP plume was encountered in the distance of ~ 7.5 km from the
22 plant at an altitude of 1900 m a.s.l. on August 21 and in the distance of ~ 5 km at 1500 – 1650
23 m a.s.l. on August 22. With a horizontal wind speed of 2.4 and 1.5 m s⁻¹ on August 21 and 22,
24 respectively, the age of the plume was ~0.9 h on both days.

25 Figures 3 and 4 show data from the flight sections with CFPP plume encounters on August 21
26 and 22, 2013, respectively. The plume encounters lasted 1 – 2 min and are clearly indicated by
27 elevated SO₂, NO_x (NO_x = NO + NO₂), and GEM concentrations measured by Lumex. CO
28 and rH enhancements are hardly visible on August 21 but are clearly recognizable on August
29 22. Tekran instruments with a temporal resolution of 150 s are too slow to resolve individual
30 plume encounters but they also show a broad peak of enhanced GEM (Tekran 1 with quartz
31 wool trap) or TGM (Tekran 2) concentrations. The difference between TGM measured by
32 Tekran 2 and GEM measured by Tekran 1 is small (on average 0.087 ± 0.117 ng m⁻³ (n = 8)



1 on August 21 and $0.063 \pm 0.079 \text{ ng m}^{-3}$ ($n = 12$) on August 22) and varies between -0.064 and
2 $+0.354 \text{ ng m}^{-3}$ on both days. The average differences are not significantly different from zero
3 and neither do the maximum and minimum differences exceed the combined uncertainty of
4 the difference of 17.7%. On August 21 the plume was encountered several times at an altitude
5 between 1600 and 2500 m a.s.l. The most pronounced encounters numbered 1 – 4 were found
6 at an altitude of 1800 – 2250 m a.s.l. On August 22 the plume was encountered 3 times at a
7 flight level of 1550 m and 3 times at 1650 m a.s.l. The numbered plume encounters were
8 selected for quantitative evaluation.

9 Figure 5 shows the vertical distribution of the values measured downwind the Lippendorf
10 CFPP. The vertical profiles above Leipzig and Waldhof are discussed together with further
11 profiles in Weigelt et al. (2016). In Figure 5 the squares represent the constant flight level
12 measurement points (2 measurements with 2.5 minutes each). The stars represent the
13 measurements when climbing between two flight levels (2.5 min average). Therefore the data,
14 indicated as squares are more significant and the data illustrated as stars do provide additional
15 information on the vertical structure. Please note that the rH, air temperature (T), and the
16 potential temperature (θ) are plotted with high temporal resolution (1 s) in the rightmost
17 panel. The rH can be used to distinguish between boundary layer- and free tropospheric air.
18 Usually inside the planetary boundary layer (PBL) the relative humidity is much higher than
19 in the free troposphere (Spencer and Braswell, 1996).

20 The lower four horizontal flight legs (570 to 1340 m a.s.l.) show typical northern hemispheric
21 GEM and TGM background concentration of $\sim 1.6 \text{ ng m}^{-3}$ without any vertical gradient. CO,
22 O₃, SO₂, as well as NO and NO₂ also show no vertical gradient, indicating a well-mixed PBL.
23 This is in agreement to the other vertical profiles measured during ETMEP-2 campaign
24 (Weigelt et al., 2016). From the fifth flight leg (1630 m a.s.l.) upward the GEM and TGM
25 concentration increases towards the PBL top (Tekran 1 (GEM): 1.7 ng m^{-3} at 1630 m a.s.l.;
26 2.6 ng m^{-3} at 1940 m a.s.l.; Tekran 2 (TGM): 1.7 ng m^{-3} at 1630 m a.s.l.; 2.8 ng m^{-3} at
27 1940 m a.s.l.; Lumex (GEM): 2.1 ng m^{-3} at 1630 m a.s.l.; 2.4 ng m^{-3} at 1940 m a.s.l.). The
28 increasing concentration is also captured by the measurements during the flight level change
29 (Tekran 1 (GEM): 1.7 ng m^{-3} at 1540 m a.s.l.; 2.1 ng m^{-3} at 1800 m a.s.l.; Tekran 2 (TGM):
30 1.7 ng m^{-3} at 1540 m a.s.l.; 2.3 ng m^{-3} at 1800 m a.s.l.; Lumex (GEM): 1.8 ng m^{-3} at 1540
31 m a.s.l.; 2.2 ng m^{-3} at 1800 m a.s.l.; stars in Fig. 5). As indicated by the abrupt decrease of rH,
32 the PBL top was found at 2150 to 2200 m a.s.l.. Therefore the flight leg 7 at 2260 m a.s.l. and



1 leg 8 at 3020 m a.s.l. were performed in free tropospheric air. These two measurements show
2 a typical free tropospheric background concentration ($\sim 1.3 \text{ ng/m}^3$, Weigelt et al., 2016 and
3 references therein). The measurements during the flight level change from leg 6 to leg 7
4 represent a mixture of boundary layer- and free tropospheric air (averaged altitude 2150 m
5 a.s.l.). Therefore the Tekran 1 GEM, Tekran 2 TGM, and Lumex GEM concentration of
6 2.3 ng m^{-3} , 2.4 ng m^{-3} , and 1.9 ng m^{-3} was strongly influenced by the high concentration
7 below the boundary layer top.

8 In the altitude range 1600 m a.s.l. to 2200 m a.s.l. not only mercury, but also SO_2 was
9 significantly increased (from 1.6 ppb to 21.4 ppb), which clearly indicates that the mercury
10 was emitted from the CFPP. Inside the plume (leg 6), the O_3 concentration was slightly
11 decreased to 42.3 ppb. At the same time NO and NO_2 increased to 6.1 ppb and 8.9 ppb,
12 respectively. Outside the plume (e.g. leg 4) O_3 was 48.5 ppb, NO was below the detection
13 limit, and NO_2 was ~ 1.5 ppb. This indicates O_3 depletion due to NO oxidation taking place
14 inside the plume (cf. Fig. 3 and 4). The presence of a temperature inversion at the PBL top is
15 indicated by the changing T and θ vertical gradient in Fig. 5. This inversion layer prevents a
16 further ascent of the power plant plume. Therefore, the highest concentration of pollutants
17 was found below the PBL top. As already shown with Fig. 3 and 4, during a flight leg in a
18 certain altitude (and during level change) the aircraft did not remain within the plume all the
19 time. Therefore, the concentrations, given in Fig. 5 do represent a mixture of plume and
20 background air.

21 The ratio of concentration enhancements (ERs), $\Delta\text{Hg}/\Delta\text{SO}_2$, $\Delta\text{Hg}/\Delta\text{CO}$, and $\Delta\text{NO}_x/\Delta\text{SO}_2$
22 represent the emission ratios at the stack if a) chemical reactions during the transport from the
23 stack to the point of interception can be neglected and b) the background concentrations have
24 not changed during the measurement including the transport from the stack to the place of
25 plume encounters. As mentioned above, the transport time from the stack to the location of
26 plume interception was ~ 0.9 h on both days. Based on OH concentrations measured in a
27 CFPP plume, Ambrose et al. (2015) estimated SO_2 and NO_x lifetimes of 16 – 43 and 1.8 – 5.8
28 h, respectively. The combination of GEM, TGM, and GOM measurements by Lumex, Tekran
29 2537X (Tekran 1, with quartz wool trap), 2537B (Tekran 2, without quartz wool trap), and
30 KCl denuder, respectively, suggests that there is no substantial conversion of GEM into GOM
31 within the transport time of ~ 0.9 h. The vertical profile over Leipzig, upwind of the CFPP,
32 was measured on August 21 ~ 3 h after the measurements in the plume. The CO, O_3 , SO_2 ,



1 NO_x and Hg concentrations in the PBL over Leipzig with ~ 120, 50, 0.5, 3 ppb, 1.4 ng m⁻³,
2 respectively, are similar to respective concentrations found outside of the plume over CFPP
3 Lippendorf. Differences between them for SO₂, NO_x, and Hg are small when compared with
4 their enhancements in the plumes of ~ 40, 30 ppb, 4 ng m⁻³, respectively. On August 22 no
5 vertical profile upwind was measured, but SO₂, NO_x, and Hg concentrations over Waldhof, ~
6 90 km north of Leipzig, measured immediately before the downwind measurements of CFPP
7 Lippendorf, were comparable. We thus conclude that the background concentrations of SO₂,
8 NO_x, and Hg have not changed significantly during the 0.9 h long transport from the stack to
9 the location of aircraft interception and during ~ 20 min of the repeated plume interceptions.
10 In addition, the large SO₂, NO_x, and Hg enhancements in the plume make the calculated
11 $\Delta\text{Hg}/\Delta\text{SO}_2$ and $\Delta\text{NO}_x/\Delta\text{SO}_2$ ERs insensitive to small changes in background SO₂, NO_x, and
12 Hg concentrations. This is not always the case for small ΔCO and negative ΔO_3 (negative
13 because O₃ is consumed by oxidation of NO to NO₂) relatively to their background mixing
14 ratios. In addition, the CO background mixing ratios changed substantially from ~123 to
15 105 ppb during the plume crossing #4 and #5 on August 21 due to altitude change. $\Delta\text{Hg}/\Delta\text{CO}$
16 for these plume interceptions was thus not calculated.

17 The ERs are usually calculated as a slope of Hg vs X correlations (e.g. Ambrose et al., 2015).
18 The advantage of this method is that the background concentrations of neither Hg nor X have
19 to be known as long as they remain constant during the measurement. The method, however,
20 is applicable only if the plume crossings are much longer than the response time of the
21 instruments. With the plume transects lasting in our case only 60 – 120 s and effective
22 temporal resolution of 10 s for SO₂ and NO_x measurements, however, the signals have to be
23 carefully synchronized. In addition, the correlation slopes for individual plume crossings will
24 become quite uncertain because of small number of points. For this reason we apply the
25 correlation method for all (synchronized) points with SO₂ mixing ratios > 10 ppb. This
26 selection provides 35 and 45 points for Hg vs SO₂ correlations on August 21 and 22,
27 respectively. Individual plume crossings are not resolved by this calculation. Correlations
28 made by the bivariate Williamson-York method (Cantrell, 2008) provide a slope and its
29 statistical uncertainty representing ER (Hg/SO₂) and its uncertainty.

30 An alternative method calculates ERs as a ratio of ΔHg to ΔX where ΔHg and ΔX are signal
31 enhancements against the background integrated over the plume crossing. This method, called
32 here “integral method”, is applicable for measurements with instruments with different



1 response times and we will show that it can use even Tekran measurements with a temporal
2 resolution of 150 s, although not for individual plume crossings. Opposite to the correlation
3 method, no exact synchronization is needed. The disadvantage, however, is that the results are
4 sensitive to the selection of background concentrations. Figures 3 and 4 show that background
5 Hg concentrations are especially difficult to define from the Lumex measurements. We thus
6 use the Hg background concentrations measured by the much more precise Tekran instrument.
7 As the Lumex instrument measured only GEM, we use the background measured by Tekran
8 instrument with quartz wool (Tekran 1). The other disadvantage of the integral method is that,
9 opposite to the correlation method, the uncertainty of ERs is difficult to quantify. We
10 overcome this difficulty here by averaging the ERs from individual plume crossings and
11 taking the standard deviation as a measure of ER uncertainty.

12 The Hg/SO₂ ERs are listed in Table 2. The correlation and integral methods provide similar
13 results with 5.53 ± 1.10 and $5.56 \pm 1.19 \mu\text{mol mol}^{-1}$, respectively, for August 21, and $7.38 \pm$
14 0.92 and $6.32 \pm 1.52 \mu\text{mol mol}^{-1}$, respectively for August 22. The integral method with Tekran
15 and SO₂ integrals over all plume encounters provide somewhat higher Hg/SO₂ ERs but still
16 within the uncertainties of the correlation and integral methods. The measured Hg/SO₂ ERs
17 are smaller than the emission ratio of $10.8 \mu\text{mol mol}^{-1}$ calculated from Hg and SO₂ annual
18 emissions reported by the operator for 2013. They are close to $5.2 - 6.5 \mu\text{mol mol}^{-1}$
19 determined by Ambrose et al. (2015) for Big Brown (BBS) and Dolet Hills Stations (DHS).
20 BBS, a 1187 MW CFPP in Texas, is fired with subbituminous coal and is equipped with
21 activated carbon injection flue cleaning. DHS, a 721 MW CFPP in Louisiana, is fired with
22 lignite and is equipped with wet flue gas desulfurization, similar to CFPP Lippendorf.

23 Hg/CO ERs are frequently used to classify the origin of different plumes (Slemr et al., 2009,
24 2014; Lai et al., 2011) with ERs $< 0.25 \mu\text{mol mol}^{-1}$ typical for plumes from biomass burning
25 and ERs $> 0.6 \mu\text{mol mol}^{-1}$ characteristic for plumes of urban/industrial origin. The Hg/CO
26 ERs measured in the plume of CFPP Lippendorf are listed in Table 3. The correlation method
27 tends to yield somewhat higher Hg/CO ERs than the integral method. Because of changing
28 background on August 21 and changing altitude on August 22, no ERs were calculated by
29 integral method using the Tekran measurements. As mentioned before, the high background
30 CO mixing ratios and relatively small CO enhancement in the plume make the integral
31 method quite sensitive to the chosen background. For this reason we believe 5.2 and $9.4 \mu\text{mol}$
32 mol^{-1} from correlation method for August 21 and August 22, respectively, to be more reliable.



1 The Hg/CO emission ratio from the 2013 annual emissions reported by the operator is 7.6
2 $\mu\text{mol mol}^{-1}$, in reasonable agreement with our measurements. Hg/CO ERs of this magnitude
3 have never been observed so far in the plumes detected during the CARIBIC flights (Slemr et
4 al., 2014). This is probably because only large plumes extending over several hundreds to few
5 thousands of km can be detected by these flights. Their Hg/CO ERs are then a mixture of
6 Hg/CO ERs from point sources embedded in plumes from larger industrial and/or urban areas.

7 Simultaneous NO_x and SO₂ measurements allow us to calculate also the NO_x/SO₂ ERs which
8 are listed in Table 4. The ERs from the correlations and integral methods are in good
9 agreement with each other on both days. The NO_x/SO₂ ER of 0.59 mol mol⁻¹ on August 21 is
10 almost twice as large as 0.27 mol mol⁻¹ on August 22, and both ERs are substantially lower
11 than the emission ratio of 0.91 mol mol⁻¹ calculated from the NO_x and SO₂ emissions reported
12 for 2013. All these NO_x/SO₂ ERs are substantially larger than ~0.08 mol mol⁻¹ reported by
13 Ambrose et al. (2015) for Big Brown CFPP in Texas and corrected for the NO_x loss during
14 the transport from the stack to the point of the plume interception.

15 Ozone is not emitted but the ambient O₃ is consumed by a rapid reaction with NO (O₃ + NO =
16 NO₂ + O₂) in the plume during the transport from the stack to the point of plume interception.
17 The O₃/NO_x ERs thus do not represent emission ratios and they are negative because of O₃
18 consumption. If only NO were emitted the O₃/NO_x ER should be -1 mol mol⁻¹. O₃/NO_x ERs
19 were not calculated for August 21 because of changing O₃ background mixing ratio. The
20 calculated O₃/NO_x ERs for August 22 are listed in Table 5. The correlation method provides a
21 slope of -0.62 ± 0.13 mol mol⁻¹ while the integral method provides an ER of -1.0 ± 0.6 mol
22 mol⁻¹. We thus conclude that the emitted NO constitute some 60 – 100% of NO_x emissions.

23

24 **4 GOM emissions**

25 As mentioned earlier the GOM measurements made here using quartz wool traps and KCl
26 denuders can be both influenced by high humidity (Huang and Gustin, 2015) and those made
27 by KCl additionally by high O₃ concentrations (Lyman et al., 2010). Because of NO
28 emissions, the O₃ concentrations in the CFPP plumes will be lower than in ambient air making
29 this interference unlikely. The humidity interference would lead to an underestimation of
30 GOM concentrations measured by KCl denuders and overestimation of GEM concentrations
31 measured by Tekran instrument with quartz wool trap. However, specific GEM measurements



1 are provided by Lumex, an atomic absorption instrument with Zeeman background correction,
2 albeit with a worse precision when compared to Tekran measurements.

3 Table 6 lists the GOM concentrations measured by the KCl denuders during the vertical
4 profiles over Leipzig and in the plume of CFPP Lippendorf on August 21, 2013, and over
5 Waldhof on August 22, 2013. Taking into account the uncertainty of $\pm 5 \text{ pg m}^{-3}$ there is hardly
6 any difference between GOM concentration of 5.8 pg m^{-3} measured during the vertical profile
7 over Leipzig and 11.4 pg m^{-3} in the plume of CFPP Lippendorf on August 21. The difference
8 of 5.6 pg m^{-3} is distributed over the vertical profile of 3000 m. Assuming $\sim 300 \text{ m}$ thick layer
9 with the CFPP plume and nearly zero GOM concentrations outside of this layer, the GOM
10 concentrations in the layer would be $\sim 60 \text{ pg m}^{-3}$. This is roughly consistent with the
11 differences between Tekran measurements without quartz wool trap and with it. The average
12 difference in the plume was $87 \pm 117 \text{ pg m}^{-3}$ ($n=8$) on August 21 and $63 \pm 79 \text{ pg m}^{-3}$ ($n=12$).
13 Related to the average TGM enhancement (Tekran without quartz wool trap) in the plume of
14 0.90 ng m^{-3} on August 21 and of 1.03 ng m^{-3} on August 22, the GOM concentration would
15 represent $\sim 10\%$ and $\sim 6\%$ of TGM emissions on August 21 and 22, respectively.

16 An independent assessment of the GOM emissions can be made using Hg/SO₂ ERs listed in
17 Table 2. On August 21, the Hg/SO₂ ER of $5.5 \pm 1.1 \text{ } \mu\text{mol mol}^{-1}$ from correlation and 5.6 ± 1.2
18 $\text{ } \mu\text{mol mol}^{-1}$ from integral methods, both based on specific GEM measurements by Lumex, are
19 within their uncertainties consistent with $6.6 \text{ } \mu\text{mol mol}^{-1}$ derived from Tekran with quartz
20 wool trap. On August 22, the Hg/SO₂ ER of $7.4 \pm 0.9 \text{ } \mu\text{mol mol}^{-1}$ from correlation method is
21 consistent with $8.1 \text{ } \mu\text{mol mol}^{-1}$ determined from Tekran data, while the $6.3 \pm 1.5 \text{ } \mu\text{mol mol}^{-1}$
22 from the integral method is somewhat lower. Consequently, Hg/SO₂ ERs from less specific
23 measurements with quartz wool trap tend to be somewhat higher but within their combined
24 uncertainties comparable with those derived from GEM specific Lumex measurements. A
25 comparison of Hg/SO₂ ERs measured by Tekran without and with quartz wool trap implies
26 GOM emissions representing 13 and 9% of TGM emissions on August 21 and 22,
27 respectively. Taking GEM specific Lumex measurements instead of those made by Tekran
28 with quartz wool trap would imply GOM emissions representing 27 and 24% on August 21
29 and 22, respectively, which we consider an upper limit.

30 In summary we conclude that GOM represents $\sim 10\%$ of the TGM emitted from CFPP
31 Lippendorf with an uncertainty range of 0 - 25%. Edgerton et al. (2006) reported GOM
32 fraction of 13, 19, and 21% of total mercury in the plumes from CFPPs Hammond, Crist, and



1 Bowen in the U.S. Stergašek et al. (2008) reported 4% GOM fraction for Hg emissions from
2 CFPP with FGD in Slovenia which was fired by lignite. Wang et al. (2010) found GOM
3 fractions of 6 -25% of all Hg emissions from five Chinese power plants with FGD. Deeds et
4 al. (2013) found 13% of total mercury being GOM in the plume of CFPP Nanticoke in
5 Canada. They think that discrepancy between this and 43% GOM fraction found in stack
6 gases is due to sampling biases. Tatum Ernest et al. (2014) support their findings using a
7 speciation technique still in development. On the other side Landis et al. (2014) report high
8 GOM fractions of > 86% in stack gases of the Crist CFPP and 4 – 40% conversion into GEM
9 in the plume in 0.6 – 1.3 km distance from the stack. They attribute the difference to a
10 reduction of GOM to GEM. Putting this unresolved issue aside, low fractions of GOM
11 emissions reported here and by others (Edgerton et al., 2006; Stergašek et al., 2008; Wang et
12 al., 2010; Deeds et al., 2013; Landis et al., 2014) are in contrast to the AMAP/UNEP
13 geospatially distributed mercury emissions dataset “2010v1” (Wilson et al., 2013), splitting
14 the speciated mercury emissions from combustion in power plants to 50% GEM, 40% GOM,
15 and 10% PBM. As mentioned before the flue gas desulphurisation (FGD) in CFPP Lippendorf
16 is made by washing of the flue gas with CaO suspension and this type of FGD is known to
17 capture most of GOM (Schütze, 2013). Although no PBM was measured in this study, 10% of
18 mercury being emitted as PBM according to the inventory is also an overestimation for CFPPs
19 with FGD (Stergašek et al., 2008; Wang et al., 2010).

20

21 **5 Conclusions**

22 Plume of the coal fired power plant (CFPP) Lippendorf near Leipzig in Germany was
23 encountered several times on August 21 and 22, 2013. On August 21 the plume was captured
24 at below planetary boundary layer top due to a temperature inversion layer. Hg/SO₂, Hg/CO,
25 NO_x/SO₂ ERs in the plume were determined as a slope of bivariate correlations of the species
26 concentrations and as ratios of integrals over the individual plume crossings. The measured
27 Hg/SO₂ and Hg/CO ERs were, within the measurement uncertainties, consistent with the ERs
28 calculated from annual emissions reported by the CFPP operator for 2013, the NO_x/SO₂ ER
29 was somewhat lower.

30 GOM fraction of total mercury emissions was estimated a) using GOM measurements by KCl
31 denuders, b) from a difference between Hg measurements by Tekran instruments without and
32 with quartz wool trap, and c) from a difference between Hg measurements by a Tekran



1 instrument without quartz wool trap and GEM specific measurements by Lumex instrument.
2 Despite large uncertainties in all these estimates we conclude that GOM emissions represent
3 ~10% of total mercury emissions with an uncertainty range of 0 – 25%. This result is
4 consistent with findings by others (Edgerton et al., 2006; Stergašek et al., 2008; Wang et al,
5 2010; Deeds et al., 2013) and suggests that GOM fractions of ~40% of CFPP mercury
6 emissions in current emission inventories are overestimated. Although PBM was not
7 measured by us, its inventoried fraction of 10% is too high too for CFPPs with FGD
8 according to the above references.

9

10 **Acknowledgements**

11 Measurements were carried out as part of the European Tropospheric Mercury Experiment
12 (ETMEP) within the Global Mercury Observation System project (GMOS; www.gmos.eu).
13 GMOS is financially supported by the European Union within the seventh framework
14 programme (FP-7, Project ENV.2010.4.1.3-2). Special thanks to Compagnia Generale
15 Ripresearee (<http://www.terraitaly.it/>) in Parma/Italy and the pilots Oscar Gaibazzi and Dario
16 Sassi for carrying out the measurement flights.

17



1 **References**

- 2 AMAP/UNEP, 2013: AMAP/UNEP geospatially distributed mercury emissions dataset
3 2010v1, available online: <http://www.amap.no/mercury-emissions/datasets> (20.11.2013)
- 4 Ambrose, J.L., Lyman, S.N., Huang, J., Gustin, M.S., and Jaffe, D.A.: Fast time resolution
5 oxidized mercury measurements during the Reno Atmospheric Mercury Intercomparison
6 Experiment (RAMIX), *Environ. Sci. Technol.*, 47, 7285-7294, 2013.
- 7 Ambrose, J.L., Gratz, L.E., Jaffe, D.A., Campos, T., Flocke, F.M., Knapp, D.J., Stechman,
8 D.M., Stell, M., Weinheimer, A., Cantrell, C., and Mauldin, R.L.: Mercury emission ratios
9 from coal-fired power plants in the southeastern U.S. during NOMADSS, *Environ. Sci.*
10 *Technol.*, 49, 10389-10397, 2015.
- 11 Amos, H.M., Jacob, D.J., Holmes, C.D., Fisher, J.A., Wang, Q., Yantosca, R.M., Corbitt,
12 E.S., Galarneau, E., Rutter, A.P., Gustin, M.S., Steffen A., Schauer, J.J., Graydon, J.A., Louis,
13 V.L.St., Talbot, R.W., Edgerton, E.S., Zhang, Y., and Sunderland, E.M.: Gas-particle
14 partitioning of atmospheric Hg(II) and its effect on global mercury deposition, *Atmos. Chem.*
15 *Phys.*, 12, 591-603, doi:10.5194/acp-12-591-2012, 2012.
- 16 Bieser, J., DeSimone, F., Gencarelli, C., Geyer, B., Hedgecock, I.M., Matthias, V., Travnikov,
17 O., and Weigelt, A.: A diagnostic evaluation of modelled mercury wet depositions in Europe
18 using atmospheric speciated high resolution observations, *Environ. Sci. Pollut. Res.*, 21,
19 9995-10012,, doi:10.1007/s11356-014-2863-2, 2014.
- 20 Cantrell, C.A.: Technical note: Review of methods for linear least-squares fitting of data and
21 application to atmospheric chemistry problems, *Atmos. Chem. Phys.*, 8, 5477-5487, 2008.
- 22 Chen, Y., Wang, R., Shen, H., Li, W., Chen, H., Huang, Y., Zhang, Y., Chen, Y., Su, S., Lin,
23 N., Liu, J., Li, B., Wang, X., Coveney Jr., R.M., and Tao, S.: Global mercury emissions from
24 combustion in light of international fuel trading, *Environ. Sci. Technol.*, 48, 1727-1735, 2014.
- 25 Deeds, D.A., Banic, C.M., Lu, J., and Daggupaty, S.: Mercury speciation in a coal-fired
26 power plant plume: An aircraft-based study of emissions from the 3640 MW Nanticoke
27 Generatin Station, Ontario, Canada, *J. Geophys. Res.*, 118, 4919-4935, 2013.
- 28 Ebinghaus, R. and Slemr, F.: Aircraft measurements of atmospheric mercury over southern
29 and eastern Germany, *Atmos. Environ.*, 34, 895-903, doi:10.1016/S1352-2310(99)00347-7,
30 2000.



- 1 Ebinghaus, R., Slemr, F., Brenninkmeijer, C. A. M., van Velthoven, P., Zahn, A., Hermann,
2 M., O'Sullivan, D. A., and Oram, D. E.: Emissions of gaseous mercury from biomass burning
3 in South America in 2005 observed during CARIBIC flights, *Geophys. Res. Lett.*, 34(8), 1–5,
4 doi:10.1029/2006GL028866, 2007.
- 5 Edgerton, E.S., Hartsell, B.E., and Jansen, J.J.: Mercury speciation in coal-fired power plant
6 plumes observed at three surface sites in the southeastern U.S., *Environ. Sci. Technol.*, 40,
7 4563-4570, 2006.
- 8 EEA (European Environmental Agency): Revealing the Costs of Air Pollution from Industrial
9 Facilities, Technical Report 15/2011, doi:10.2800/84800, Copenhagen, 2011.
- 10 Friedli, H. R., Radke, L.F., Prescott, R., Li, P., Woo, J.-H., and Carmichael, G.R.: Mercury in
11 the atmosphere around Japan, Korea, and China as observed during the 2001 ACE-Asia field
12 campaign: Measurements, distributions, sources, and implications, *J. Geophys. Res.*,
13 109(D19), 1–13, doi:10.1029/2003JD004244, 2004.
- 14 EPA (Environmental Protection Agency): Electric Generating Utility Mercury Speciation
15 Profiles for the Clean Air Mercury Rule, EPA-454/R-11-010, November 2011. Available
16 online:
17 https://www3.epa.gov/ttn/chief/emch/speciation/EGU_Hg_speciation_summary_CAMR.pdf
- 18 Gustin, M.S., Huang, J., Miller, M.B., Peterson, C., Jaffe, D.A., Ambrose, J., Finley, B.D.,
19 Lyman, S.N., Call, K., Talbot, R., Feddersen, D., Mao, H., and Lindberg, S.E.: Do we
20 understand what the mercury speciation instruments are actually measuring? Results of
21 RAMIX, *Environ. Sci. Technol.*, 47, 7295-7306, 2013.
- 22 Gustin, M.S., Amos, H.M., Huang, J., Miller, M.B., and Heidekorn, K.: Measuring and
23 modelling mercury in the atmosphere: a critical review, *Atmos. Chem. Phys.* 15, 5697-5713,
24 2015.
- 25 Huang, J., and Gustin, M.S.: Uncertainties of gaseous oxidized mercury measurements using
26 KCl-coated denuders, cation-exchange membranes, and nylon membranes: Humidity
27 influences, *Environ. Sci. Technol.*, 49, 6102-6108, doi:10.1021/acs.est.5b00098, 2015.
- 28 Jaffe, D.A., Lyman, S., Amos, H.M., Gustin, M.S., Huang, J., Selin, N.E., Levin, L., ter
29 Schure, A., Mason, R.P., Talbot, R., Rutter, A., Finley, B., Laeglé, L., Shah, V., McClure, C.,
30 Ambrose, J., Gratz, L., Lindberg, S., Weiss-Penzias, P., Sheu, G.-R., Feddersen, D., Horvat,
31 M., Dastoor, A., Hynes, A.J., Mao, H., Jonke, J.E., Slemr, F., Fisher, J.A., Ebinghaus, R.,



- 1 Zhang, Y., and Edwards, G.: Progress on understanding atmospheric mercury hampered by
2 uncertain measurements, *Environ. Sci. Technol.*, 48, 7204-7206, doi:10.1021/es5026432,
3 2014.
- 4 Kaiser, R., and Gottschalk, G.: *Elementare Tests zur Beurteilung von Meßdaten*,
5 Hochschultaschenbücher, Band 774, Bibliographisches Institut, Mannheim, 1972.
- 6 Kos, G., Ryzhkov, A., Dastoor, A., Narayan, J., Steffen, A., Ariya, P.A., and Zhang, L.:
7 Evaluation of discrepancy between measured and modelled oxidized mercury species, *Atmos.*
8 *Chem. Phys.*, 13, 4839-4863, doi:10.5194/acp-13-4839-2013, 2013.
- 9 Lai, S.C., Baker, A.K., Schuck, T.J., Slemr, F., Brenninkmeijer, C.A.M., van Velthoven, P.,
10 Oram, D.E., Zahn, A., and Ziereis, H.: Characterization and source regions of 51 high-CO
11 events observed during the Civil Aircraft for the Regular Investigation of the atmosphere
12 Based on the Instrument Container (CARIBIC) flights between South China and the
13 Philippines, 2005-2008, *J. Geophys. Res.*, 116, D20308, doi:10.1029/2011JD016375, 2011.
- 14 Landis, M.S., Ryan, J.V., ter Schure, A.F.H., and Laudal, D.: Behavior of mercury emissions
15 from a commercial coal-fired power plant: The relationship between stack speciation and
16 near-field plume measurements, *Environ Sci. Technol.*, 48, 13540-13548, 2014.
- 17 Lindberg, S., Bullock, R., Ebinghaus, R., Engstrom, D., Feng, X., Fitzgerald, W., Pirrone, N.,
18 Prestbo, E. and Seigneur, C.: A synthesis of progress and uncertainties in attributing the
19 sources of mercury in deposition, *AMBIO*, 36, 19-33, 2007.
- 20 Lohman, K., Seigneur, C., Edgerton, E., and Janssen, J.: Modeling mercury in power plant
21 plumes, *Environ, Sci. Technol*, 40, 3848-3854, 2006.
- 22 Lyman, S.N., Jaffe, D.A., and Gustin, D.S.: Release of mercury halides from KCl denuders in
23 the presence of ozone, *Atmos. Chem. Phys.*, 10, 8197-8204, doi:10.5194/acp-10-8197-2010,
24 2010.
- 25 Mason, R.P.: Mercury emissions from natural processes and their importance in the global
26 mercury cycle, in *Mercury Fate and Transport in the Global Atmosphere*, eds. Pirrone, N.,
27 and Mason, R., Springer Dordrecht, 2009, pp. 173-191.
- 28 Mayer, J., Hopf, S., van Dijen, F., and Baldini, A.: Measurement of low mercury
29 concentrations in flue gases of combustion plants, *VGB PowerTech Journal*, 3/2014, 64-68,
30 2014.



- 1 Mergler, D., Anderson, H.A., Chan, L.H.N., Mahaffey, K.R., Murray, M., Sakamoto, M., and
2 Stern, A.H.: Methylmercury exposure and health effects in humans: A worldwide concern,
3 *Ambio*, 36, 3-11, 2007.
- 4 Pacyna, E. G., Pacyna, J. M., Steenhuisen, F., and Wilson, S.: Global anthropogenic mercury
5 emission inventory for 2000, *Atmos. Environ.*, 40, 4048 – 4063, 2006.
- 6 Pirrone, N., Cinnirella, S., Feng, X., Finkelman, R. B., Friedli, H. R., Leaner, J., Mason, R.,
7 Mukherjee, A. B., Stracher, G. B., Streets, D. G. and Telmer, K.: Global mercury emissions to
8 the atmosphere from anthropogenic and natural sources, *Atmos. Chem. Phys.*, 10, 5951–5964,
9 doi:10.5194/acp-10-5951-2010, 2010.
- 10 Preiss, P., Roos, J., and Friedrich, R.: *Assessment of Health Impacts of Coal Fired Power*
11 *Stations in Germany*, report by the Institute for Energy Economics and Rational Use of
12 Energy (IER), University of Stuttgart, March 29th, 2013.
- 13 Radke, L. F., Friedli, H. R. and Heikes, B. G.: Atmospheric mercury over the NE Pacific
14 during spring 2002: Gradients, residence time, upper troposphere lower stratosphere loss, and
15 long-range transport, *J. Geophys. Res.*, 112(D19), 1–17, doi:10.1029/2005JD005828, 2007.
- 16 Rutter, A.P., and Schauer, J.J.: The effect of temperature on the gas-particle partitioning of
17 reactive mercury in atmospheric aerosols, *Atmos. Environ.*, 41, 8647-8657, 2007.
- 18 Scheele, M. P., Siegmund, P. C. and van Velthoven, P. F. J.: Sensitivity of trajectories to data
19 resolution and its dependence on the starting point: In or outside a tropopause fold, *Meteorol.*
20 *Appl.*, 3(3), 267–273, doi:10.1002/met.5060030308, 2007.
- 21 Scheuhammer, A.M., Meyer, M.W., Sandheinrich, M.B., and Murray, M.W.: Effects of
22 environmental methylmercury on the health of wild birds, mammals, and fish, *Ambio*, 36, 12-
23 18, 2007.
- 24 Schofield, K.: Fuel-mercury combustion emissions: An important heterogeneous mechanism
25 and an overall review of its implications, *Environ. Sci. Technol.*, 42, 9014-9030,
26 doi:10.1021/es801440g, 2008.
- 27 Schuetze, J., Kunth, D., Weissbach S., and Koeser, H.: Mercury vapor pressure of flue gas
28 desulfurization scrubber suspensions: Effects of pH level, gypsum, and iron, *Environ. Sci.*
29 *Technol.*, 46, 3008-3012, doi:10.1021/es203605h, 2012.



- 1 Schütze, J.: *Quecksilberabscheidung in der nassen Rauchgasentschwefelung von*
2 *Kohlekraftwerken*, Beiträge zum Umweltschutz, Band 6/2013, Shaker Verlag, Aachen, 2013.
- 3 Selin, N. E.: Global biogeochemical cycling of mercury: A review, *Ann. Rev. Environ.*
4 *Resour.*, 34, 43–63, doi:10.1146/annurev.enviro.051308.084314, 2009.
- 5 Sholupov, S., Pogarev, S., Ryzhov, V., Mashyanov, N., and Stroganov, A.: Zeeman atomic
6 absorption spectrometer RA-915+ for direct determination of mercury in air and complex
7 matrix samples, *Fuel Process. Technol.*, 85, 473-485, 2004.
- 8 Slemr, F., Seiler, W., and Schuster, G.: Quecksilber in der troposphere, *Ber. Bunsenges. Phys.*
9 *Chem.*, 82, 1142-1146, 1978.
- 10 Slemr, F., Seiler, W., Eberling, C., and Roggendorf, P.: The determination of total gaseous
11 mercury in air at background levels, *Anal. Chim. Acta.*, 110, 35-47, 1979.
- 12 Slemr, F., Ebinghaus, R., Brenninkmeijer, C.A.M., Hermann, M., Kock, H.H., Martinsson,
13 B.G., Schuck, T., Sprung, D., van Velthoven, P., Zahn, A., and Ziereis, H.: Gaseous mercury
14 distribution in the upper troposphere and lower stratosphere observed onboard the CARIBIC
15 passenger aircraft, *Atmos. Chem. Phys.*, 9, 1957-1969, 2009.
- 16 Slemr, F., Weigelt, A., Ebinghaus, R., Brenninkmeijer, C., Baker, A., Schuck, T., Rauthe-
17 Schöch, A., Riede, H., Leedham, E., Hermann, M., van Velthoven, P., Oram, D., O’Sullivan,
18 D., Dyroff, C., Zahn, A. and Ziereis, H.: Mercury plumes in the global upper troposphere
19 observed during flights with the CARIBIC observatory from May 2005 until June 2013,
20 *Atmosphere (Basel)*, 5(2), 342–369, doi:10.3390/atmos5020342, 2014.
- 21 Slemr, F., Weigelt, A., Ebinghaus, R., Kock, H.H., Bödewadt, J., Brenninkmeijer, C.A.M.,
22 Rauthe-Schöch, A., Weber, S., Hermann, M., Becker, J., Zahn, A., and Martinsson, B.:
23 Atmospheric mercury measurements onboard the CARIBIC passenger aircraft, *Atmos.*
24 *Measur. Techn. Discuss.*, doi:10.594/amt-2015-376, 2016.
- 25 Spencer, R. W. and Braswell, W. D.: How dry is the tropical free troposphere ? Implications
26 for global warming theory, *Bull. Am. Meteorol. Soc.*, 78, 1097–1106, doi:10.1175/1520-
27 0477(1997)078<1097:HDITTF>2.0.CO;2, 1996.
- 28 Stergašek, A., Horvat, M., Kotnik, J., Tratnik, J., Frkal, P., Kocman, D., Jaćimović, R., Fajon,
29 V., Ponikvar, M., Hrstel, I., Lenart, J., Debeljak, B., and Čujež, M.: The role of flue gas



- 1 desulphurisation in mercury speciation and distribution in a lignite burning power plant, *Fuel*,
2 87, 3504-3512, 2008.
- 3 Swartzendruber, P. C., Jaffe, D. A., Prestbo, E. M., Weiss-Penzias, P., Selin, N. E., Park, R.,
4 Jacob, D. J., Strode, S. and Jaeglé, L.: Observations of reactive gaseous mercury in the free
5 troposphere at the Mount Bachelor Observatory, *J. Geophys. Res.*, 111,
6 doi:10.1029/2006JD007415, 2006.
- 7 Swartzendruber, P. C., Chand, D., Jaffe, D. A., Smith, J., Reidmiller, D., Gratz, L., Keeler, J.,
8 Strode, S., Jaeglé, L. and Talbot, R.: Vertical distribution of mercury, CO, ozone, and aerosol
9 scattering coefficient in the Pacific Northwest during the spring 2006 INTEX-B campaign, *J.*
10 *Geophys. Res.*, 113, doi:10.1029/2007JD009579, 2008.
- 11 Swartzendruber, P. C., Jaffe, D. A. and Finley, B.: Development and first results of an
12 aircraft-based, high time resolution technique for gaseous elemental and reactive (oxidized)
13 gaseous mercury, *Environ. Sci. Technol.*, 43(19), 7484–7489, doi:10.1021/es901390t, 2009.
- 14 Tatum Ernest, C., Donohue, D., Bauer, D., Ter Schure, A., and Hynes, A.J.: Programmable
15 thermal dissociation of reactive gaseous mercury, a potential approach to chemical speciation:
16 Results from a field study, *Atmosphere*, 5, 575-596, doi:10.3390/atmos5030575, 2014.
- 17 Wang, S.X., Zhang, L., Li, G.H., Wu, Y., Hao, J.M., Pirrone, M., Sprovieri, F., and Ancora,
18 M.P.: Mercury emission and speciation of coal-fired power plants in China, *Atmos. Chem.*
19 *Phys.*, 10, 1183-1192, 2010.
- 20 Weigelt, A., Temme, C., Bieber, E., Schwerin, A., Schuetze, M., Ebinghaus, R. and Kock, H.
21 H.: Measurements of atmospheric mercury species at a German rural background site from
22 2009 to 2011 – methods and results, *Environ. Chem.*, 10(2), 102–110, doi:10.1071/EN12107,
23 2013.
- 24 Weigelt, A., Ebinghaus, R., Pirrone, N., Bieser, J., Bödewadt, J., Esposito, G., Slemr, F., van
25 Velthoven, P.F.J., Zahn, A., and Ziereis, H.: Tropospheric mercury vertical profiles between
26 500 and 10000 m in central Europe, *Atmos. Chem. Phys.*, 16, 4135-4146, 2016.
- 27 Weiss-Penzias, P., Amos, H.M., Selin, N.E., Gustin, M.S., Jaffe, D.A., Obrist, D.,
28 Sheu, G.-R., and Giang, A.: Use of a global model to understand speciated
29 atmospheric mercury observations at five high-elevation sites, *Atmos. Chem. Phys.*,
30 15, 2225-2225, doi:10.5194/acp-15-2225-2015, 2015.



- 1 Wilson, S., Munthe, J., Sundseth, K., Kindbom, K., Maxson, P., Pacyna, J., and
2 Steenhuisen, F.: *Updating Historical Global Inventories of Anthropogenic Mercury Emissions*
3 *to Air*. Arctic Monitoring and Assessment Programme (AMAP) Technical Report No. 3.,
4 AMAP Secretariat, Oslo; Norway, 2010.
- 5 Wilson, S., Kindbom, K., Yaramenka, K., Steenhuisen, F., Telmer, K., and Munthe, J.: Global
6 emission of mercury to the atmosphere, in AMAP/UNEP, *Technical Background Report for*
7 *the Global Mercury Assessment*, Arctic Monitoring and Assessment Programme, Oslo,
8 Norway/UNEP Chemicals Branch, Geneva, Switzerland, 2013.
- 9 Zhang, L., Blanchard, P., Gay, D.A., Presbo, E.M., Risch, M.R., Johnson, D., Narayan, J.,
10 Zsolway, R., Holsen, T.M., Miller, E.K., Castro, M.S., Graydon, J.A., St. Louis, V.L., and
11 Dalziel, J.: Estimation of speciated and total mercury dry deposition at monitoring locations
12 in eastern and central North America, *Atmos. Chem. Phys.*, 12, 4327-4340, 2012a.
- 13 Zhang Y., Jaegle L., van Donkelaar A., Martin R.V., Holmes C.D., Amos, H.M., Wang, Q.,
14 Talbot, R., Artz, R., Brooks, S., Luke, W., Holsen, T.M., Felton, D., Miller, E.K., Perry, K.D.,
15 Schmeltz, D., Steffen, A., Tordon, R., Weiss-Penzias, P., and Zsolway, R.: Nested-grid
16 simulation of mercury over North America, *Atmos. Chem. Phys.*, 12, 6095-6111,
17 doi:10.5194/acp-12-6095-2012, 2012b.
- 18



1 Tables

2 Table 1: List of instruments, installed into the CASA 212 research aircraft. The acronyms are:

3 GEM = gaseous elemental mercury; GOM = gaseous oxidized mercury.

Parameter	Instrument name	Temporal resolution	Uncertainty	Lower detection limit
GEM	Lumex RA-915AM (modified, T-stabilised by Lumex company)	1 sec (raw signal)	$\pm 4 \text{ ng/m}^3$ (1 s raw signal) $\pm 1 \text{ ng/m}^3$ (10 s average)	0.5 ng/m^3 (120 s average)
GEM	Tekran: 2537X (with upstream quartz wool trap)	150 s	$\pm 12.5\%$ of reading	$0.1 \text{ ng}\cdot\text{m}^{-3}$
GEM + unknown amount of GOM*	Tekran 2537B	150 s	$\pm 12.5\%$ of reading	$0.1 \text{ ng}\cdot\text{m}^{-3}$
GOM	manually denuder samples	2600 to 3600 s	$\pm 5 \text{ pg}\cdot\text{m}^{-3}^{**}$	$1 \text{ pg}\cdot\text{m}^{-3}$
CO	Aero Laser AL5002	1 s	$\pm 3\%$ of reading	1.5 ppb
O ₃	Teledyne API 400E	10 s	$\pm 2\%$ of reading	0.6 ppb
SO ₂	Thermo: 43C Trace Level	10 s	$\pm 4\%$ of reading	0.2 ppb
NO NO ₂	Teledyne API M200AU	10 s 10 s	$\pm 10\%$ of reading	0.05 ppb
Pressure	Sensor Technics CTE7001	1 s	$\pm 1\%$ of reading	0 mbar
Temperature	LKM Electronic DTM5080	1 s	$\pm 0.13^\circ\text{C}$	-50°C
Relative Humidity (rH)	Vaisala HMT333	8 s	$\pm 1.0\%$ rH (0-90% rH) $\pm 1.7\%$ rH (90-100% rH)	0%
GPS data (3d position, speed, heading)	POS AV	1 s	$\pm 5 \text{ m}$ (horizontal)*** $\pm 15 \text{ m}$ (vertical)***	---

4 * The aircraft inlet system transmission efficiency for GOM was not tested because no GOM sources
 5 were available which would enable measurements during the flight.

6 ** Difference of the two blank tests

7 *** The GPS accuracy is dependent on the number of satellites. The given numbers are estimated
 8 values.



1 Table 2: Hg/SO₂ enhancement ratios (ERs). Correlation method: 10 s average Hg
 2 concentrations measured by Lumex correlated with 10 s average SO₂ mixing ratios, only Hg
 3 values with SO₂ concentrations > 10 ppb were taken, uncertainties set to 1 ng m⁻³ for Lumex
 4 and 0.5 ppb for SO₂. Integral method: 1 s Lumex and SO₂ signals integrated over the duration
 5 of Lumex measurement, –measurements of Tekran with quartz wool taken as Lumex
 6 background concentrations (i.e. 1.27 and 1.25 ng m⁻³ for August 21 and 22, respectively). SO₂
 7 background mixing ratio was 0.83 and 0.66 ppb on August 21 and 22, respectively.

Date	Method	Species	ER 10 ⁻⁶ mol mol ⁻¹	n, R, signif	Comment
August 21, 2013	correlation	GEM	5.53 ± 1.10	35, 0.6564, >99.9%	
	integral peak 1	GEM	6.67		Lumex zeroing
	integral peak 2	GEM	5.72		
	integral peak 3	GEM	5.98		Lumex zeroing
	integral peak 4	GEM	3.88		
	integral peak 5	GEM	0.89		
	integral average	GEM	5.56 ± 1.19*	4*	
	Tekran with quartz wool trap	GEM	6.56		
	Tekran	TGM	7.55		
August 22, 2013	correlation	GEM	7.38 ± 0.92	45, 0.7751, >99.9%	
	integral peak 1	GEM	6.44		
	integral peak 2	GEM	4.83		
	integral peak 3	GEM	5.90		Lumex zeroing
	integral peak 4	GEM	6.67		
	integral peak 5	GEM	9.03		Lumex zeroing
	integral peak 6	GEM	5.02		
	integral average	GEM	6.32 ± 1.52	6	
	Tekran with quartz wool trap	GEM	8.13		
Tekran	TGM	8.97			
2013	reported annual emissions	TGM	10.8		

8

9 * average without integral of peak 5 which is identified as outlier by Nalimov test (at >95%
 10 significance level, Kaiser and Gottschalk, 1972)

11



1

2 Table 3: Hg/CO enhancement ratios (ERs). Correlation method: 10 s average Hg
 3 concentrations measured by Lumex correlated with 10 s average CO mixing ratios for SO₂
 4 mixing ratios above 10 ppb, uncertainties set to 1 ng m⁻³ for Lumex and 1 ppb for CO.
 5 Integral method: 1 s Lumex and CO signals integrated over the duration of Lumex
 6 measurement, Tekran 1 readings taken as Lumex background concentrations (i.e. 1.27 and
 7 1.25 ng m⁻³ for August 21 and 22, respectively). CO background mixing ratio was 119.3 ppb
 8 on August 21 and 123.8 ppb on August 22.

Date	Method	ER (Hg/CO)		Comment
		10 ⁻⁵ mol mol ⁻¹	n, R, signif	
August 21, 2013	Correlation	5.19 ± 0.94	31, 0.6596, >99.9%	values only until 10:40:20
	integral peak 1	3.40		Lumex zeroing
	integral peak 2	4.16		
	integral peak 3	3.33		Lumex zeroing
	integral peak 4			background change
	integral peak 5			CO calibration
	integral average	3.63 ± 0.46	3	
August 22, 2013	Correlation	9.43 ± 1.07	37, 0.7880, >99.9%	
	integral peak 1	3.19		
	integral peak 2			CO calibration
	integral peak 3			Lumex zeroing, CO calibration
	integral peak 4	7.87		
	integral peak 5	5.61		Lumex zeroing
	integral peak 6	4.75		
integral average	5.36 ± 1.95	4		
2013	reported annual emissions	7.58		

9

10



1 Table 4: NO_x/SO₂ enhancement ratios (ERs). Correlation method: 10 s average NO_x mixing
 2 ratios correlated with 10 s average SO₂ mixing ratios above 10 ppb, uncertainties set to 1 ppb
 3 for NO_x and 0.5 ppb for SO₂. Integral method: 1 s NO_x and 1 s SO₂ signals integrated over
 4 the duration of the individual plume intersection, background mixing ratios for SO₂ and NO_x
 5 are 0.83 and 1.78 ppb, respectively, for August 21 and 0.66 and 0.45 ppb, respectively for
 6 August 22.

Date	Method	ER (NO _x /SO ₂) mol mol ⁻¹	n, R, signif	Comment
August 21, 2013	Correlation	0.585 ± 0.038	34, 0.9379, >99.9%	
	integral peak 1	0.598		
	integral peak 2	0.575		
	integral peak 3	0.725		
	integral peak 4	0.497		
	integral peak 5			
	integral average	0.598 ± 0.095	4	
August 22, 2013	Correlation	0.262 ± 0.051	40, 0.6344, >99.9%	
	integral peak 1	0.297		
	integral peak 2	0.457		
	integral peak 3	0.167		Lumex zeroing
	integral peak 4	0.330		
	integral peak 5	0.133		Lumex zeroing
	integral peak 6	0.317		
	integral average	0.284 ± 0.118	6	
2013	reported annual emissions	0.910		

7

8

9

10



1 Table 5: O₃/NO_x enhancement ratios (ERs). Correlation method: 10 s average O₃ mixing
 2 ratios correlated with 10 s average SO₂ mixing ratios above 10 ppb, uncertainties set to 1 ppb
 3 for O₃ and 1 ppb for NO_x. Integral method: 1 s O₃ and 1 s NO_x signals integrated over the
 4 duration of the individual plume intersection, background mixing ratios for O₃ and NO_x are
 5 43.09 and 1.78 ppb, respectively, for August 21. Individual O₃ background mixing ratios
 6 (average of background before and after the peak) varying between 53.9 ppb for peak 1 to
 7 56.2 ppb for peak 4 were taken for August 22. The NO_x background mixing ratio on August
 8 22 was 0.45 ppb.

Date	Method	ER (O ₃ /NO _x)	n, R, signif	Comment
August 22, 2013	Correlation	-0.620 ± 0.134	40, -0.3776, >95%	
	integral peak 1	-0.979		
	integral peak 2	-0.424		
	integral peak 3	-1.527		
	integral peak 4	-0.686		
	integral peak 5	-2.059		
	integral peak 6	-0.568		
	integral average	-1.040 ± 0.633	6	

9

10



1 Table 6: Results of the manual KCl denuder samples during all ETMEP-2 measurement
 2 flights in 2013 over central Europe. GOM data were corrected for denuder blank test,
 3 additionally performed over Iskraba/Slovenia and Waldhof/Germany. GOM concentrations
 4 are given as a centre of an estimated uncertainty range (in brackets) and are given at standard
 5 temperature and pressure (STP; T=273.15 K, p=1013.25 hPa).

6

Date	Location	Profile character (relative sampling time in PBL* and FT** air	analysed GOM concentration [μg m^{-3}]
2013-08-21	Lippendorf/Germany	vertical (76% PBL; 24% FT)	11.4 (7.0-15.7)
2013-08-21	Leipzig/Germany	vertical (61% PBL; 39% FT)	5.8 (1.0*** - 10.6)
2013-08-22	Waldhof/Germany	vertical (54% PBL; 46% FT)	31.0 (24.6-37.3)

7 * planetary boundary layer (PBL)

8 ** free troposphere (FT)

9 ***If a concentration was found to be below the method lower detection limit of $1.0 \mu\text{g m}^{-3}$,
 10 the lower detection limit is given.

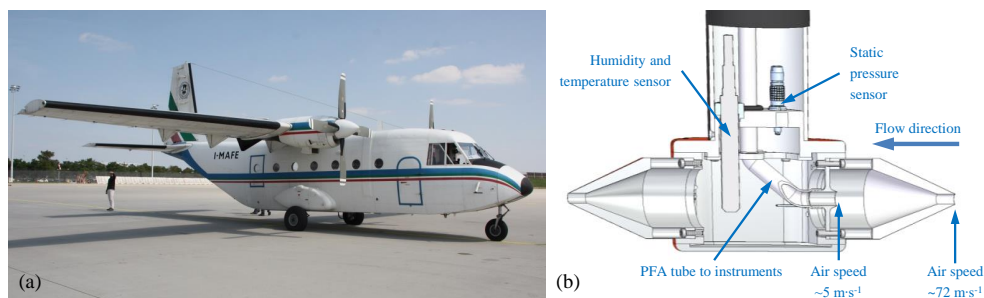
11

12



1 **Figures**

2

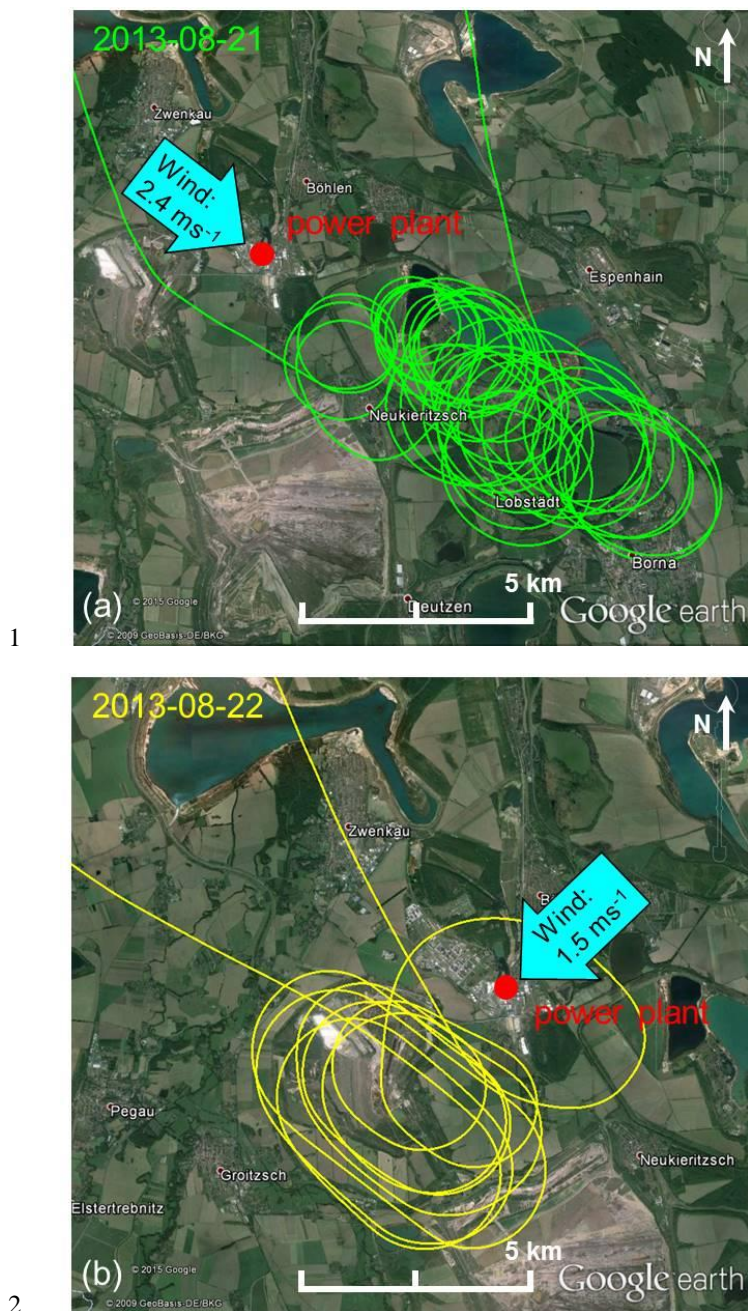


3

4

5 Figure 1: For the ETMEP-2 campaign in August 2013 the CASA 212 (a) from the Italian
6 company Compagnia Generale Ripresearee (<http://www.terraitaly.it/>) was equipped with
7 specially designed and manufactured trace gas inlet (b).

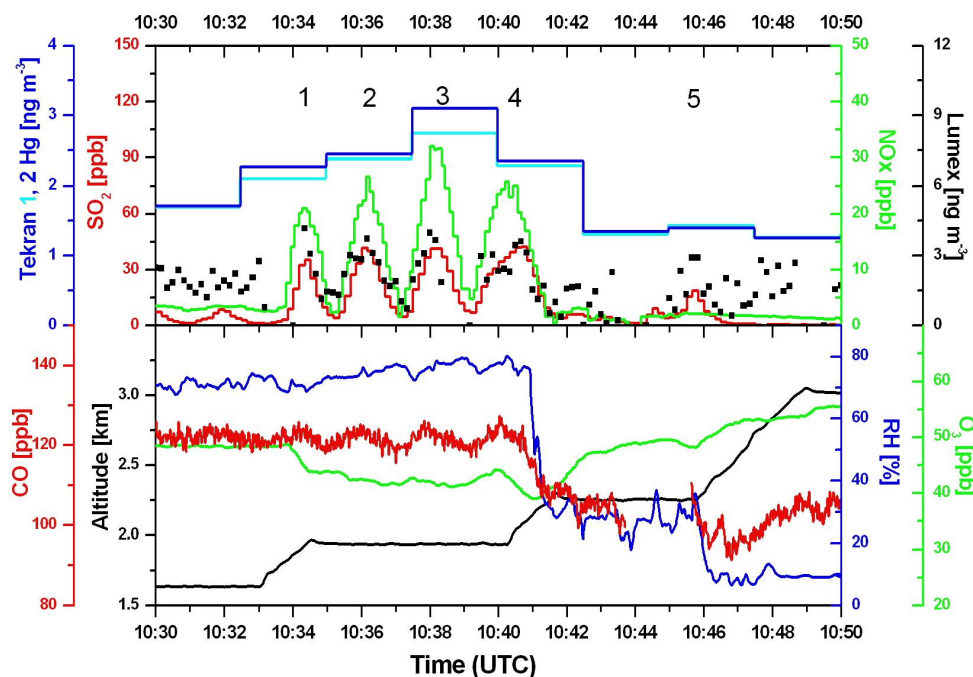
8



3 Figure 2: Flight track of the ETMEP-2 flights on August 21 (a) and 22 (b), 2013 downwind
4 the coal fired power plant “Lippendorf”, south of Leipzig, Germany. On both flights the
5 power plant plume was crossed several times.



1



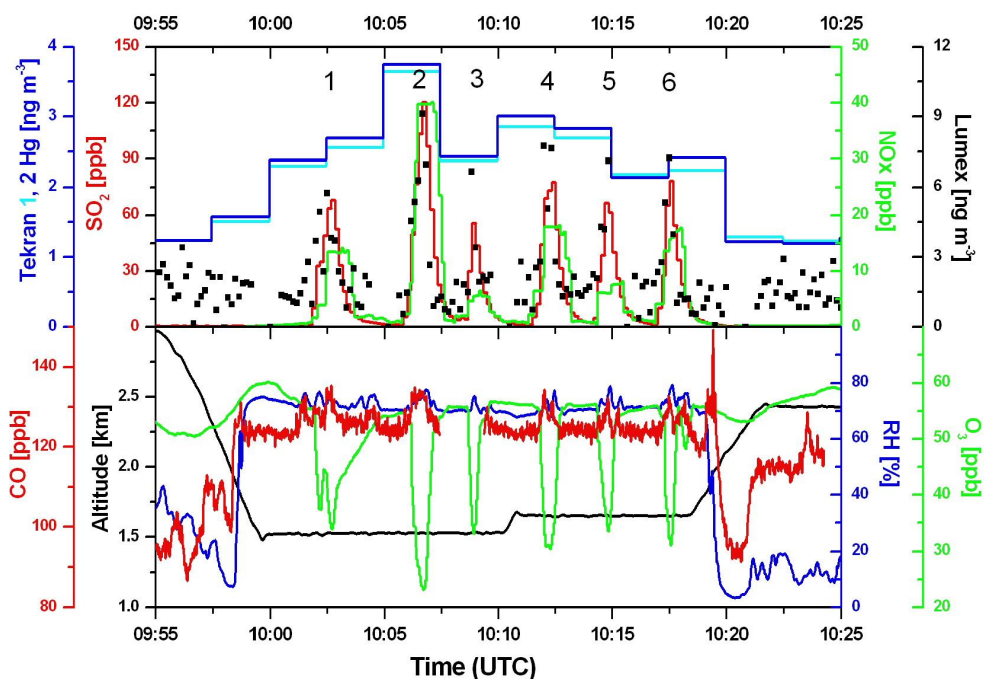
2

3

4 Figure 3: ETMEP-2 coal fired power plant plume measurements on August 21, 2013 south of
5 Leipzig/Germany. The gaps in the Lumex signal (10 s resolution) are due to internal zero air
6 checks for the correction of the instruments base line drift. Tekran 1 was run with quartz wool
7 trap at the inlet of the instrument presumed to remove GOM, Tekran 2 without. Tekran 1 and
8 2 measurements are thus presumed to represent GEM and TGM measurements, respectively.
9 All parameters were synchronized using individual instrument delay and response times. All
10 Hg concentrations are given at standard temperature and pressure (STP; $T=273.15$ K,
11 $p=1013.25$ hPa).

12

13



1

2

3 Figure 4: ETMEP-2 coal fired power plant plume measurements on August 22, 2013 south of
4 Leipzig/Germany. The gaps in the Lumex signal (10 s resolution) are due to internal zero air
5 checks for the correction of the instruments base line drift. Tekran 1 was run with quartz wool
6 trap at the inlet of the instrument presumed to remove GOM, Tekran 2 without. Tekran 1 and
7 2 measurements are thus presumed to represent GEM and TGM measurements, respectively.
8 All parameters were synchronized using individual instrument delay and response times. All
9 Hg concentrations are given at standard temperature and pressure (STP; $T=273.15$ K,
10 $p=1013.25$ hPa).

11

12

13

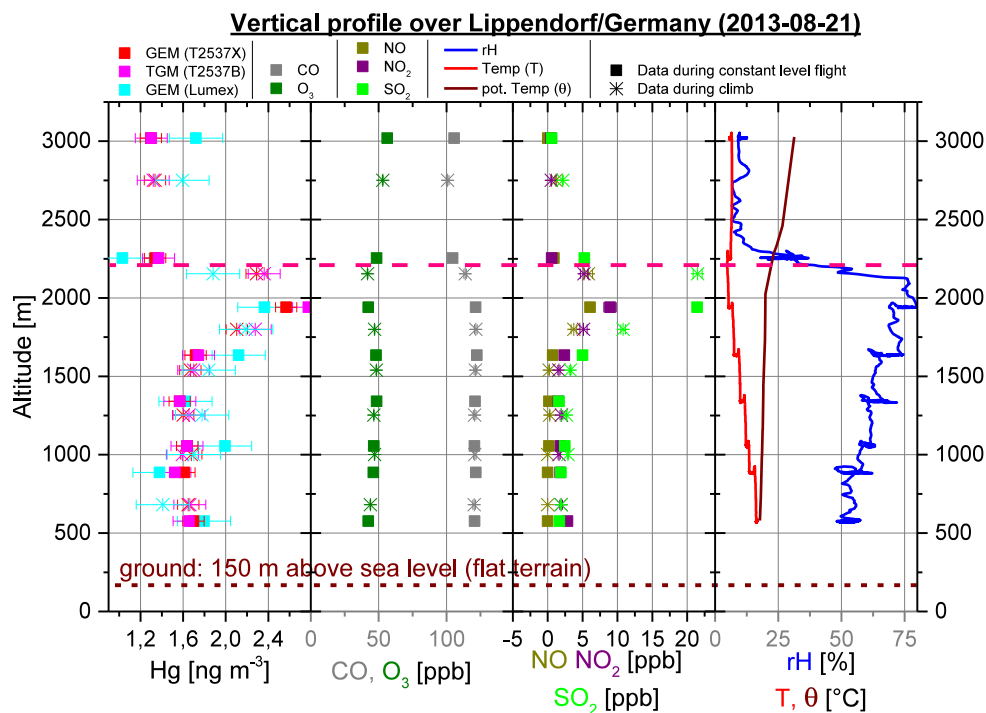
14

15



1

2



3

4 Figure 5: Vertical profile, measured on 21 August 2013 from 13:17:30 to 14:07:30 (local
5 time) downwind the coal fired power plant Lippendorf (central Germany; 45.561°N,
6 14.858 °E, elevation: 150 m a.s.l.; flat terrain). Squares represent 300 s averages with
7 horizontal flight leg; stars indicate 150 s averages during climbing between two neighbouring
8 flight legs. The red dashed line indicates the planetary boundary layer (PBL) top, which was
9 determined to be at 2150 to 2250m a.s.l.. All Hg concentrations are given at standard
10 temperature and pressure (STP; T=273.15 K, p=1013.25 hPa).